KINGDOM OF SAUDI ARABIA
Northern Border University (NBU)
Journal of the North for Basic & Applied Sciences(JNBAS)
p - ISSN : 1658 -7022 / **e-ISSN:** 1658 - 7014
www.nbu.edu.sa
s.journal@nbu.edu.sa

DFT studies of the geometry, electronic structure and vibrational spectra of some 1,3-Benzothiazole derivatives

Ali A. El-Rayyes
Chemistry Department, Faculty of Science, Northern Border University, Arar 1321, Saudi Arabia.

(Received: 09/01/2024; Accepted: 05/03/2024)

Abstract: Calculated geometrical parameters for some 1,3-benzothiazole derivatives (1,3-BT), namely; 2-vinyl-1,3-benzothiazole, 2-(2-pyridyl)-1,3-benzothiazole, 1,3-benzothiazole-2-carboxaldehyde and 1,3-benzothiazole- 2-carbonyl fluoride were calculated using density functional theory (DFT) at the 6-311++G(d,p) level. Excited state calculations were carried out using the Time Dependent-DFT/6-311++G(d,p) method. 1,3-BT is found to exist in two main conforms, the A form and the B form with the B form to be more stable than the A form with A form to B form rotational barrier ranging from 5.73 Kcal/mol to 9.78 Kcal/mol. HOMO-LUMO energies and the global quantum chemical parameters were determined. For substituted 1,3-BT molecules, the energy difference between HOMO and LUMO was determined to be between 4.70 and 3.95 eV. Both vinyl and formyl substituted BT have the highest and lowest values of η that is 2.35 and 1.98 eV, respectively. Simulated UV and IR spectra were determined with complete assignments of the vibrational frequencies.

Keywords: DFT calculations; Rotational barrier; Vibrational frequencies and spectra, 1,3-benzothiazole derivatives, 2-(2-Pyridyl)-1,3-benzothiazole.

DOI: 10.12816/0062033

(*) **Corresponding Author**:
Ali A. El-Rayyes, Chemistry Department, Faculty of Science, Northern Border University, Saudi Arabia.
Arar: 1321
E-mail: ali.elrayyes@nbu.edu.sa

المملكة العربية السعودية
جامعة الحدود الشمالية (NBU)
مجلة الشمال للعلوم الأساسية والتطبيقية (JNBAS)
طباعة ردمد: 1658-7022 / إلكتروني - ردمد: 1658-7014
www.nbu.edu.sa
http://jnbas.nbu.edu.sa

دراسة الشكل و التركيب الالكتروني واطياف الاهتزاز لبعض مشتقات مركب 1و-3بنزوثيازول بواسطة نظرية الكثافة الوظيفية

د.علي الريس
جامعة الحدود الشمالية، كلية العلوم، قسم الكيمياء – عرعر – المملكة العربية السعودية

(قدم للنشر في 2024/01/09؛ وقبل للنشر في 2024/3/05)

مستخلص البحث: تم التعرف على الاشكال الفراغية لبعض مشتقات 1,3-بنزوثيازول (1,3-BT) وهي؛ 2-فينيل-1،3-بنزوثيازول، 2-(2-بيريديل)-1،3-بنزوثيازول، 1،3-بنزوثيازول-2-كربوكسالدهيد و1،3-بنزوثيازول-2-كربونيل فلوريد باستخدام نظرية الكثافة الوظيفية (DFT) عند المستوى 6-311++G(d,p). تم إجراء حسابات الحالة المثارة باستخدام طريقة Time Dependent-DFT/6-311++G(d,p). تم العثور على 1،3-BT في اثنين من المتناظرات الفراغية، A form & B form ليكون B-form أكثر استقرارًا من الشكل A form مع حاجز الدوران الذي يتراوح من 5.73 كيلو كالوري / مول إلى 9.78 كيلو كالوري / مول. تم تحديد أطياف الأشعة فوق البنفسجية وطاقات HOMO-LUMO و التي تراوحت بين 4.70 و3.95 الكترون فولت وبعض الثوابت الكيميائية الكمومية العالمية، على سبيل المثال الثابت η له قيم تتراوح بين 2.35 و1.98 لكل من مشتق الفينيل و الفورميل. تم تحديد أطياف الأشعة تحت الحمراء المحاكاة مع تعيينات كاملة للترددات الاهتزازية.

كلمات مفتاحية: حسابات نظرية الكثافة الوظيفية، حاجز الدوران، ترددات واطياف الاهتزاز، مشتقات مركب 1و3-بنزوثيازول، 2(2-بيرديل) 1و3-بنزوثيازول

(*) للمراسلة:
د.علي الريس، جامعة الحدود الشمالية، كلية العلوم، قسم الكيمياء، عرعر، المملكة العربية السعودية.
عرعر: 1321
E-mail: ali.elrayyes@nbu.edu.sa

DOI: 10.12816/0062033

1. Introduction

Heterocyclic compounds such as benzothiazoles (BT) constituents two fused rings of thiazole and benzene (Téllez,López-Sandoval,Silvia,Castillo-Blum,Barba-Behrens, 2008). Organic and medicinal chemists have been fascinated by benzothiazole and its derivatives as potential pharmaceuticals. Benzothiazole possesses a wide range of biological actions, including anti-inflammatory, anti-tumor, anti-HIV, anti-virus, schistosomicidal, anti-bacterial, and anti-tumor properties.

The benzothiazole molecule has two distinct chromophores: aromatic rings and thiazole. These chromophores have intriguing chemical and biological features that encourage further study of the compounds. Numerous studies on substituted benzothiazoles have revealed a range of biological activity and chemical reactivity. Pharmacological activity such as antiviral (Mubarik, Mahmood, Rasool, Hashmi, Ammar, Mutahir, Ali, Bilal, Akhtar, Ashraf, (2022), antibacterial (Sathyanara, Karunathan, Kannappan, 2013), antimicrobial (Hafizi, Zainal, Mark-lee, Tahir, Ahmad, Kassim, 2018), and fungicidal (Mabrouk, Azazi, Alimi, 2010), are reported for the benzothiazole ring. As anti-allergic (Zahradník,1990), antidiabetic (Bédé, Koné, Kon, Ouattara, Ouattara, Bamba, 2019), anticancer (Tahlan, Kumar, Narasimhan 2019), anti-inflammatory (Chen, Femia, Babich, Zubieta, 2001), anthelmintic (Tariq, Kamboj, Amir 2019), and anti-HIV agents, they are also beneficial. Moreover, condensed pyrimido-benzothiazoles and benzothiazolo-quinazolines exhibit antiviral action, while phenyl substituted benzothiazoles have anticancer activity (Khokr, Arora, Kha, Kaushik, Saini, Husain, 2019; Mishra, Ghanavatkara, Malib, Qureshi, Chaudhari, Sekar, 2019; Yagodzinska, Yagodzinski, Yablonski, 1980).

Computational chemistry has emerged as a fascinating field in recent years for using a laptop or other modern computer to analyze chemical problems (Singhal, Mishra, Datta, 2016; Maji, Sengupta, Chattopadhyay, Mostafa, Schwalbe & Ghosh, 2001; Coni, Massacesi, Ponticelli, Puggioni & Putzolu, 1987; Malik, Manvi, Nanjwade, Singh, Purohit, 2010; Gomathi, Vijayan, Viswanathamurthi, Suresh, Nandhakumar & Hashimoto, 2017; Melnik, Mikuš & Holloway, 2013; Kuramshina, Vakula, Vakula, Majouga, Senyavin, Gorb, Leszczynski, 2016). It is a rapidly developing and informative field that works with the mathematical calculation and visualization of systems, including pharmaceuticals, polymers, biomolecules, and organic and inorganic complexes and molecules.

Due to their distinctive electro-optical properties, these heterocyclic compounds containing electron-rich nitrogen and sulfur heteroatoms have received a lot of attention in recent years (Mishra, Ghanavatkara, Malib, Qureshi, Chaudhari, Sekar, 2019). In addition to their biological and pharmacological features (Malik1, Manvi, Nanjwade, Singh, Purohit, 2010; Tong, Fu, Ma,2018; Niknam, Hamidizadeh, Nabavizadeh, Niroomand, Hoseini, Ford, Abu-Omar, 2019; He, Vogels, Decken , Westcott, 2004), benzothiazole derivatives may produce a spectrum of colors with good transport properties, which makes them suitable for application in light-emitting diodes (LEDs) as both emissive and electron-transporting materials (Maji, Sengupta, Chattopadhyay, Mostafa, Schwalbe & Ghosh, 2001).

Due to the lack of experimental determination of structure and geometries of some 2-substituted 1,3-benzothiazole (1,3-BT), The present study is to theoretically investigate the geometrical structures, conformations and spectroscopic properties of 2-vinyl-1,3-benzothiazole (VBT), 2-(2-pyridyl)-1,3-benzothiazole (PBT), 1,3-benzothiazole-2-carboxaldehyde (BTC) and 1,3-benzothiazole-2-carbonyl fluoride (BTCF). Density functional theory (DFT) have been used to perform the gas phase calculations for the molecules under study at both ground and excited states. Results of the study could enable researchers to closely look at these molecules as a potential precursor in the preparation of new electro-optical materials.

2. COMPUTATIONAL METHOD

All of the computations have been performed using the density functional theory (DFT) technique, which is included in the Gaussian 09 program package (Frisch et al, 2003). Previous research has demonstrated that the molecular geometry, vibrational frequency, and electrical characteristics of organic molecules have been accurately and consistently determined using DFT methods (Dennington, Keith, & Semichem, 2016; Jamroz, 2004; El-Rayyes, Umar, 2005; El-Rayyes, Maung, 2005; El-Rayyes, Maung, 2004). The calculations in this study were performed utilizing the 6-311G++(d,p) basis set by applying the B3LYP method (El-Rayyes, 2003; El-Rayyes, 2003). GaussView (Dennington, Keith, & Semichem, 2016) was used to create the initial geometries of the molecules under study. After that, unrestricted geometry optimization and frequency calculations were performed. Figure 1 shows the atom numbering in 1,3-BT molecules.

Further calculations, such as electronic parameter, vibrational infrared spectra, and UV-visible spectra of the molecules, were subsequently performed using the newly optimized structural parameters. The electronic absorption spectra were performed using time-dependent density functional theory (TD-DFT) . Using the polarizable continuum model (PCM) and its integral equation formalism variant (IEF-PCM), the UV-visible spectral calculations were performed in methanol (Umar and El-Rayyes, 2024). Based on the potential energy

distribution as previously mentioned (El-Rayyes, Umar, 2005; El-Rayyes, Maung, 2005; El-Rayyes, Maung, 2004; El-Rayyes, 2003; El-Rayyes, 2003; Umar and El-Rayyes, 2024)], normal vibrational modes were identified using the VEDA4 program (Jamroz, 2004). For Gaussian software calculations a z-matrix describing the molecular geometries is used as a data input file, however, for VEDA 4 program the optimized frequescies obtained from DFT calculations is used as input data file.

2.1 Asymmetric torsional potential function

By allowing N=C–CC (N=C–CO in formyl and N=C–CN in the pyridyl derivative) torsional angle (φ) to vary by 15° increments from 0° (A form, where the vinyl double bond (or the carbonyl group) eclipses the N=C bond) to 180° (B form, where the vinyl double bond (or the carbonyl group) is anti to the N=C bond), the potential surface scan for the internal rotation about the C–C single bond was obtained. After identifying the saddle areas, geometry optimization was performed at the transition states. Furthermore, geometry optimization was performed at each of the fixed torsional angles (φ) [N=C–CC (N=C–CO or N=C–CN)] at 15, 30, 45, 75, 90, 105, 135, 150, and 165. The torsional potential was represented as a Fourier cosine series in the dihedral angle (φ):

$$V(\phi) = V_0 + \sum_n \left({}^{V_n}/_2\right)[1 - COS(n\phi)]$$

; where the potential coefficients from V1 to V6 are thought to be sufficient to explain the potential function, and V0 is the relative energy of the A form. Using the recursive least squares method, the six coefficients were determined based on the energy optimization results that correspond to (φ) of 0°–180°. Table 1 contains a list of the data. Figure 2 displays the asymmetric potential functions for the internal rotation of the four molecules.

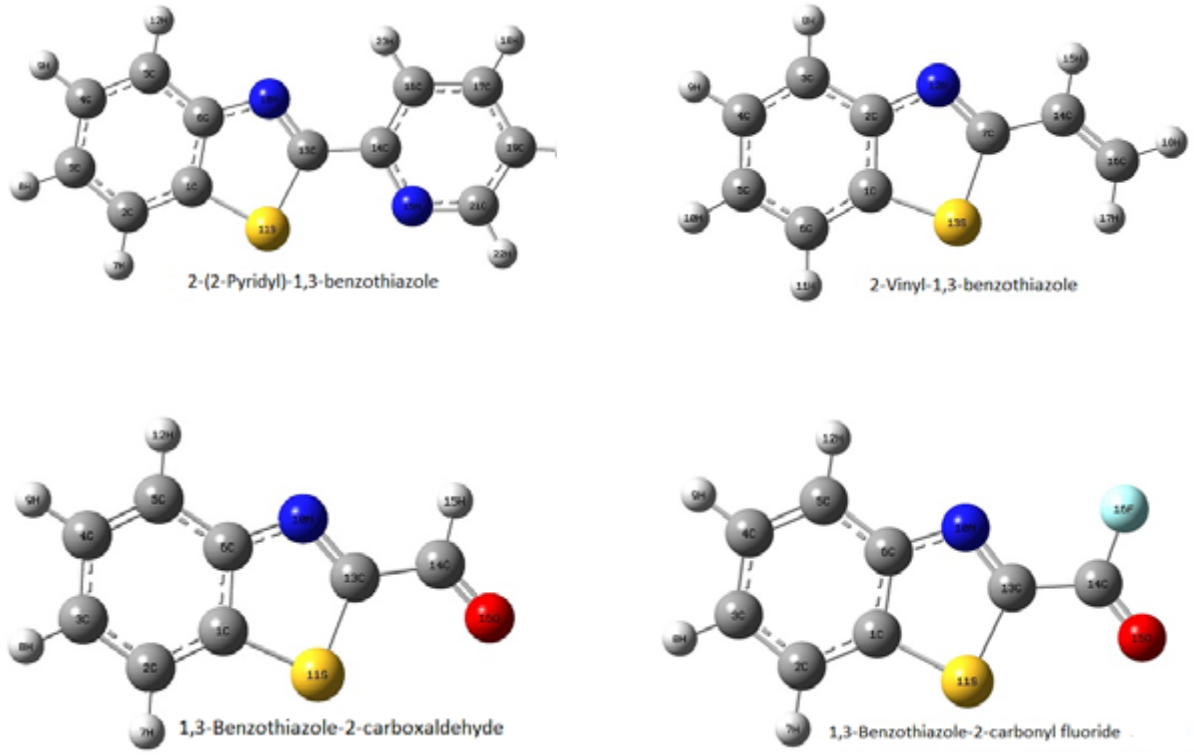

Figure 1: Atom numbering for optimized structures of 1,3-benzothiazole derivatives

3. RESULT

3.1 Molecular geometries:

The DFT-B3LYP optimized geometry parameters for the most stable geometrical structure of the molecules are given in Table 2. The C-C bond lengths were calculated to be in the range of 1.457–1.480 Å, depending on the substituent with the least value found in VBT (1.457 Å) and the highest value in PBT (1.480 Å) indicating more π-bond character in case of VBT. The C=N bond length of thiazole ring varies from 1.294 Å in COF substituent 1.341 Å in 2-pyridyl substituent. This is mainly attributed to the charge effect. The slightly longer values in 2-pyridyl derivative indicated more single bond character due to resonating structures.

When hetero aromatic ring bond distances are compared, it becomes clear that due to differences in electronegativities between substituents and associated atoms the bond distances in hetero aromatic rings are diverging dramatically from one another. The S–C7 bond length is longer than S-C1 bond distance, with higher values found in the longest pyridyl derivative (1.793 Å) and shortest value found with COF substituted BT is 1.768 Å indicating pure single bond. While S-C1 bond length varies from 1.750 Å to 1.745 Å, an average distance for a carbon–sulfur bond and the 1.81 Å which indicate that the actual bond order is between one and two which is due to conjugative effect in benzothiazole. For N=C and N-C2 bond lengths, due to ring strain the N=C double bond distance is 1.297 Å, 1.291 Å, 1.298 Å and 1.294 Å in VBT, PBT, BTC and BTCF respectively.

Symmetry of the thiazole ring is distorted due to substitution effect, yielding ring angles smaller than 120° at the point of substitution. This fact was clear from the calculated S-C-N bond angle in VBT, BTC and BTCF, while it was exactly found to equal 120° in PBT, this suggests a planar configuration due to conjugation between thiazole ring and pyridyl substituent.

Compared to the benzene ring, the heteroring exhibits greater distortion in bond properties. The central atom's electronegativity, the existence of a lone pair of electrons, and the conjugation of the double bonds all affect how much the bond angle varies. The bond angle decreases with decreasing core atom electronegativity. Thus, the bond angle C–S–C is very less (88.6°, 88.6°, 87.9° and 87.9°) in VBT, PBT, BTC and BTCF respectively, than the bond angle C–N–C (111.9°, 112.0°, 111.0°, 110.8°) in VBT, PBT, BTC and BTCF respectively, which is due to the fact that electronegativity of nitrogen is greater than sulfur.

3.2 Energetics

The B3LYP total energies of the four molecules, VBT, PBT, BTC and BTCF in their stable conformations is summarized in Table 3. Free rotation of the C-C bond lead to an equilibrium between the A form and B form with the B form to be the most stable conformation The corrected barrier to interconversion, A form-B form barrier was found to be about 5.005 kcal/mol, 7.435 kcal/mol, 5.058 kcal/mol and 5.390 kcal/mol in VBT, PBT, BTC and BTCF respectively. The high rotational barrier is a result of the possible conjugation where the C-C single bond could have some π-character. This could be explained in terms of electronic effects, where the electron donating vinyl group lead to more delocalized double bond.

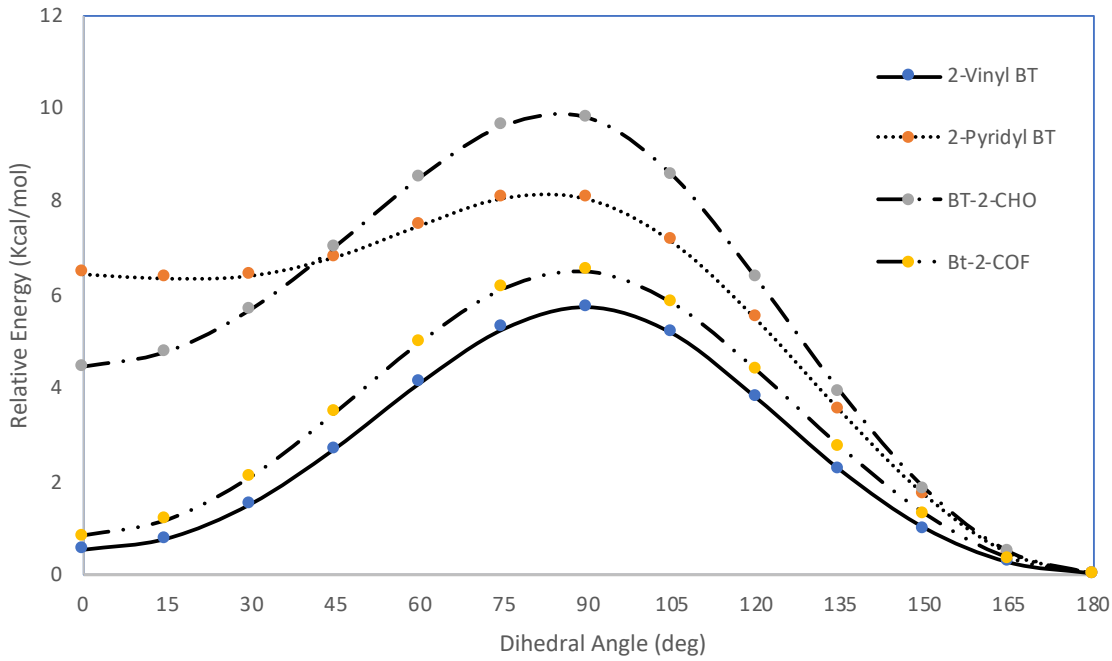

Figure 2: The determined potential surface for 2-vinyl-1,3-benzothiazole (solid line), 2-(2-pyridyl)-1,3-benzothiazole (dotted line), 1,3-benzothiazole-2-carboxaldehyde (dashed line) and 1,3-benzothiazole-2-carbonyl fluoride(dashed-dotted line)

Table 1. Calculated potential coefficients (kcal/mol) for internal rotation in substituted 1,3-BT derivatives calculated at DFT-B3LYP/6-311++G(d,p) level

Parameter	2-Vinyl-1,3-benzothiazole	2-(2-Pyridyl)-1,3-benzothiazole	1,3-Benzothiazole-2-carboxaldehyde	1,3-Benzothiazole-2-carbonyl fluoride
V_1	-0.787	-0.897	-4.352	-0.416
V_2	4.946	5.747	3.100	1.822
V_3	-0.450	-0.520	0.193	0.034
V_4	-0.293	-0.329	-0.293	-0.137
V_5	0.129	0.138	0.129	0.019
V_6	0.021	0.019	0.021	0.038

Table 2. Optimized parameters for substituted1,3-BT derivatives calculated at B3LYP /6-311++G(d,p) level of theory

Parametera	2-Vinyl-1,3-benzothiazole	2-(2-Pyridyl)-1,3-benzothiazole	1,3-Benzothiazole-2-carboxaldehyde	1,3-Benzothiazole-2-carbonyl fluoride
Bond distance (A°)				
R(C=C)	1.336	1.402		
R(C-C)	1.457	1.480	1.477	1.476
R(C=N)	1.297	1.341	1.298	1.294
R(C7-S13)	1.787	1.793	1.768	1.768
R(N-C2)	1.380	1.291	1.376	1.375
R(S13-C1)	1.750	1.747	1.747	1.745
R(C1-C2)	1.414	1.451	1.418	1.418
R(C=O)			1.209	1.188
R(C-F)				1.348
Valence angles (deg)				
∠(SC7N12)	115.0	120.3	116.4	116.6
∠(CSC)	88.6	88.6	87.9	87.9
∠(C7NC2)	111.9	112.0	111.0	110.8
∠(C=C-C7)	126.3	122.2		
∠(C-C-S)	122.3	120.3	121.1	118.3
∠(C-C-N)	122.7	124.9	122.5	125.0
∠(O=C=C)			123.9	126.3
∠(OCH)			122.8	121.6
Dihedral Angles (deg)				
∠(CCCN)	180.0	180.0		
∠(CCCS)	0.0	0.0		
∠(OCCN)			180.0	180.0
∠(OCCS)			0.0	0.0
Rotational Constant (MHz)				
A	2843.8	1877.7	2868.0	2284.8
B	659.3	297.2	655.4	529.1
C	535.2	256.6	533.5	429.6
Dipole Moment (Debye)				
μ	1.09	1.40	3.83	5.25

[a] Atom numbering are provided in Figure 1

Table 3: Computed total energies and/or zero-point corrections (hartrees), and relative energy and rotational barriers (kcal/mol) in 2-substituted benzothiazole calculated at DFT-B3LYP/6-311++G)d,p) level

	2-Vinyl-1,3-benzothiazole	2-(2-Pyridyl)-1,3-benzothiazole	1,3-Benzothiazole-2-carboxaldehyde	1,3-Benzothiazole-2-carbonyl fluoride
Total energy				
cis	-800.2322566	-969.9601537	-836.1577691	-935.4510216
trans	-800.2330631	-969.9703854	-836.1648137	-935.451216
TS	-800.2239564	-969.9575511	-836.1492803	-935.4419881
Relative energy	0.508	6.446	4.438	0.818
cis–trans Barrier	5.229	1.640	5.348	5.691
trans–cis Barrier	5.737	8.086	9.786	6.509
Zero-point correction				
cis	0. 092902	0.064529	0.049464	0.112754
trans	0.092925	0.064508	0.049553	0.112759
TS	0.093258	0.064018	0.049925	0.113230
Corrected relative energy	0.494	6.359	4.382	0.815
Corrected cis–trans barrier	5.005	1.318	5.058	5.390

3.3 Electronic Properties and Energy Profile

The highest occupied molecular orbitals (HOMO) and the lowest unoccupied molecular orbitals (LUMO) three-dimensional graphs for the four benzothiazole compounds obtained via optimization and frequency calculations are shown in Figure 3. The electronic characteristics of the four benzothiazole compounds, including oscillator strengths and excitation energies, were calculated using the TD-DFT/IEFPCM method. The HOMO and LUMO patterns and their energies are displayed in Figure 3. The absorption spectra of the four benzothiazole compounds are displayed in Figure 4. Every molecule has a unique absorption peak in the methanol medium. The electron transfer from the ground state to the excited state is correlated with the associated excitation energy of each absorption peak.

The most likely absorption wavelengths for benzothiazoles are listed in Table 4, along with the principal molecular orbital contributions, oscillator strengths, and molecular orbital assignments that correspond to them in the methanol medium. The electron transfer from the ground state to the excited state is correlated with the associated excitation energy of each absorption peak. The most likely absorption wavelengths for benzothiazoles are listed in Table 4, along with the principal molecular orbital contributions, oscillator strengths, and molecular orbital assignments that correspond to them.

The electronic excitation wavelengths of the envisioned spectra were found to be between 228 and 370 nm, as shown in Figure 4. It is clear that the different absorption wavelengths of the BT compounds are caused by the unique electronic characteristics of the substituent. The HOMO and LUMO energy values are used to determine the global reactivity descriptors, which include ionization potentials (IP), hardness (η), chemical potential (μ), chemical softness (S), and the electrophilicity index (ω). The global reactivity descriptors and the calculated HOMO, LUMO, and HOMO-LUMO energy values are shown in Table 5.

The lowest energy electronic excitation permitted in the molecules under study, recognized as the HOMO-LUMO energy gap, which is the difference between the HOMO and LUMO energies. The electrons ability to move determines how energy is distributed properly across the molecule in large conjugated systems, stabilizing it. Therefore, a lower HOMO-LUMO energy gap suggests a more chemically stable system. The energy difference between HOMO and LUMO for BT molecules was found to be between 4.70 and 3.95 eV. With an energy gap of 4.70 eV, the vinyl derivative is considered to have more chemically stable structure than the formyl derivative, which has the least stable structure with HOMO-LUMO energy gab of 3.95 eV, as seen in Table 5.

Table 4: Calculated absorption wavelength (λ), excitation energies (E), and oscillator strengths (f) for substituted1,3-BT derivatives at TD-DFT/B3LYP/6–311++ G(d,p)

	l(nm)	E(eV)	f	cont	Assignments*
2-Vinyl-1,3-benzothiazole	303	4.09	0.0645	68	42 -> 43
	282	4.40	0.5112	66	41 -> 43
	261	4.74	0.0001	99	40 -> 43
	240	5.16	0.0003	76	42 ->45
	234	5.30	0.0391	46	42 -> 44
	229	5.41	0.0005	78	41 -> 45
2-(2-Pyridyl)-1,3-benzothiazole	l(nm)	E(eV)	f	cont	Assignments*
	316	3.92	0.5937	86	55 -> 56
	309	4.01	0.0835	79	54 -> 56
	299	4.14	0.0305	89	53 -> 56
	270	4.58	0.0124	66	52 -> 56
	268	4.62	0.0209	72	55 -> 57
	266	4.65	0.0038	82	53 -> 57
1,3-Benzothiazole-2-carboxaldehyde	l(nm)	E(eV)	f	cont	Assignments*
	370	3.35	0.0271	79	42 -> 43
	361	3.44	0.0096	67	40 -> 43
	324	3.82	0.3810	85	41 -> 43
	301	4.11	0.0362	84	39 -> 43
	246	5.05	0.0074	89	38 -> 43
	229	5.41	0.0268	43	42 -> 45
1,3-Benzothiazole-2-carbonyl fluoride	l(nm)	E(eV)	f	cont	Assignments*
	367	3.38	0.0342	96	46 -> 47
	323	3.84	0.3446	86	45 -> 47
	304	4.07	0.0801	87	44 -> 47
	272	4.57	0.0001	94	42 -> 47
	244	5.08	0.0125	89	43 -> 47
	228	5.43	0.0474	51	46 -> 50

2-Vinyl-1,3-benzothiazole	**LUMO**	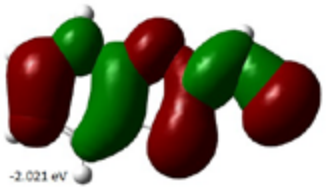
	HOMO	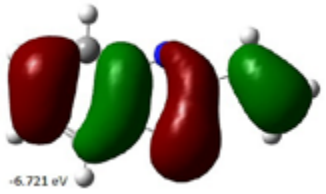
2-(2-pyridyl)-1,3-benzothiazole	**LUMO**	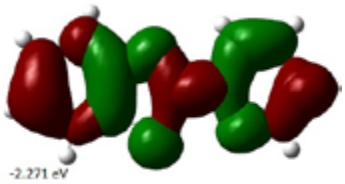
	HOMO	
1,3-benzothiazole-2-carboxaldehyde	**LUMO**	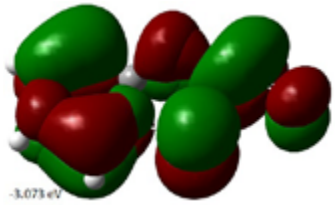
	HOMO	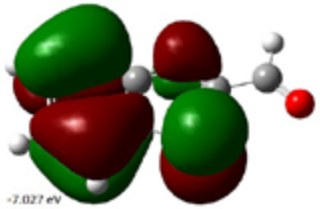
1,3-benzothiazole- 2-carbonyl fluoride	**LUMO**	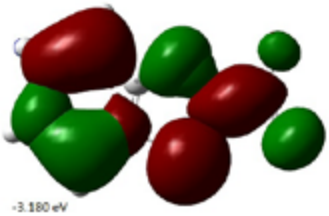
	HOMO	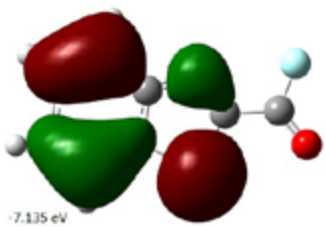

Figure 3. HOMO and LUMO patterns for substituted1,3-BT derivatives calculated by B3LYP/6–311++G(d,p).

The HOMO and LUMO energies can be used to calculate many quantum chemical properties, such as electronegativity (χ), chemical hardness (η), softness (s), potential (μ), and electrophilicity (ω). Since it evaluates the resistance to charge transfer, the η, which represents the molecule's propensity for charge transfer, is an effective means for validating chemical processes [Umar and El-Rayyes, 2024)]. The highest and lowest values of η for substituted BT are 2.35 and 1.98 eV, for vinyl and formyl substituted BT respectively. Given this, it is easy to determine that the softest molecule that is most prone to chemical reactions and charge transfer is formyl BT.

A molecule with a higher χ value is an electron acceptor that is superior to other molecules. The vinyl and COF derivatives have the lowest and highest values' χ values have been determined to be 4.37 and 5.16 eV, respectively. The high χ values linked to COF derivatives may be primarily caused by the presence of fluoride atoms. The alkenyl and aryl groups' ability to donate electrons is the primary cause of the fall in χ parameter values observed in both vinyl and pyridyl derivatives.

The electrophilicity index (ω) classifies systems according to their capacity of taking away electrons from their environment in order to take up additional electronic charge. The BT molecules substituted with CHO and COF have the largest ω parameter, measuring 6.45 and 6.72 eV, respectively.

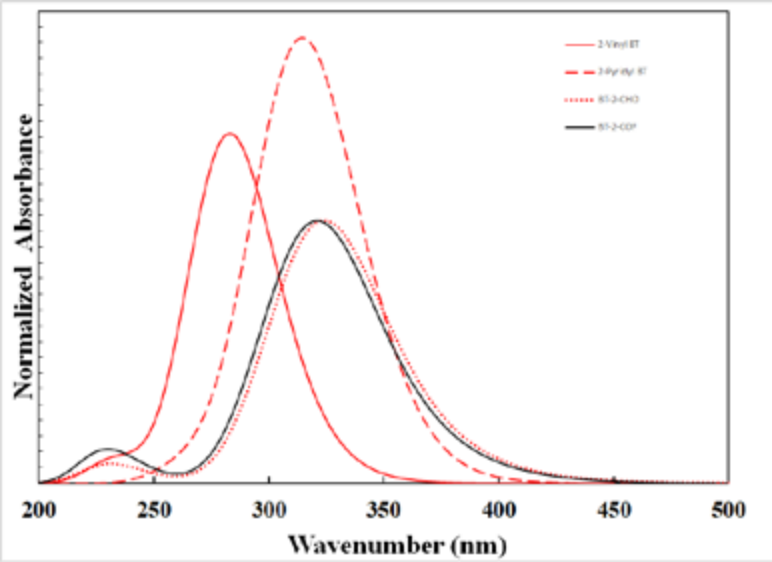

Figure 4: UV spectra of substituted 1,3-benzothiazole molecules.

Table 5 Calculated HOMO and LUMO energies, HOMO-LUMO energy gap, and global reactivity descriptors for substituted 1,3-BT

Propertya	2-Vinyl-1,3-benzothiazole	2-(2-Pyridyl)-1,3-benzothiazole	1,3-Benzothiazole-2-carboxaldehyde	1,3-Benzothiazole-2-carbonyl fluoride
EHOMO (eV)	-6.7210	-6.6571	-7.0274	-7.1346
ELUMO (eV)	-2.0207	-2.2705	-3.0726	-3.1796
|ΔE | = EHOMO - ELUMO gap (eV)	4.70	4.39	3.95	3.96
Ionization potentials (I)	6.72	6.66	7.03	7.13
Electron affinity (A)	2.02	2.27	3.07	3.18
Electronegativity (χ)	4.37	4.46	5.05	5.16
Chemical hardness (η)	2.35	2.19	1.98	1.98
Chemical potential (μ)	-4.37	-4.46	-5.05	-5.16
Chemical softness (S),	0.21	0.23	0.25	0.25
Electrophilicity index (ω)	4.06	4.54	6.45	6.72

[a] **$I = -E_{HOMO}$ (eV), $A = -E_{LUMO}$ (eV), $\chi = (I + A)/2$ (eV), $\eta = (I - A)/2$ (eV), $\mu = -(I + A)/2$ (eV), $S = 1/(2\eta)$ (eV^{-1}), $\omega = \mu^2/2\eta$(eV)**

3.4 Vibrational IR spectral properties

For the more stable conformer, the B form conformer, figure 5 shows the calculated vibrational spectra for the molecules and tables 6 and 7 include the determined vibrational wavenumbers and their associated intensities as well as the proposed vibrational mode assignments.

3.4.1 C–H Stretching

Owing to aromatic C–H stretching vibrations, Aromatic compounds are known to exhibit numerous weak bands in the 3100–3000 cm−1 area (Tariq, Kamboj, Amir 2019; Khokr, Arora, Kha, Kaushik, Saini, Husain, 2019; Mishra, Ghanavatkara, Malib, Qureshi, Chaudhari, Sekar, 2019; Yagodzinska, Yagodzinski, Yablonski, 1980). The C–H stretching vibrations in the current case are recorded between 3200 and 3140 cm−1. In benzothiazoles, an experimental Ar-CH stretching vibration of 3056 cm-1 has been reported (Mishra, Ghanavatkara, Malib, Qureshi, Chaudhari, Sekar, 2019). The region between 1300 and 1000 cm−1 is where the aromatic C–H in-plane bending modes of benzene and its derivatives are detected. The medium intensity C–H out-of-plane bending modes (Tariq, Kamboj, Amir 2019; Khokr, Arora, Kha, Kaushik, Saini, Husain, 2019; Mishra, Ghanavatkara, Malib, Qureshi, Chaudhari, Sekar, 2019; Yagodzinska, Yagodzinski, Yablonski, 1980; Singhal, Mishra, Datta, 2016), often capture in the 950–600 cm−1 range. When it comes to BT, the bands that are seen between 1200 and 960 cm−1 are attributed to the C–H in-plane bending vibrations. Within the range of 1000–600 cm−1, the C–H out of plane bending mode of benzene derivatives is detected. The medium to weak bands found at 1014 and 978 cm−1 in the infrared spectrum is assigned to the aromatic C–H out of plane bending vibrations of BT. There is a significant overlap between the in-plane and out-of-plane ring C–C–C bending modes and the aromatic C–H bending vibrations.

3.4.2 C–S Stretching

Because of their high polarizability, the C–S bonds exhibit greater spectral activity. The predicted range for the C–S stretching vibration is 710–685 cm−1 (Khokr, Arora, Kha, Kaushik, Saini, Husain, 2019). Benzothiazoles were found to exhibit C-S stretching vibrations with an experimental value of 706 -672 cm−1 (Yagodzinska, Yagodzinski, Yablonski, 1980). For the molecules under investigation, the C–S stretching vibrations have been identified in the 682–714 cm−1 area. The computed frequencies of 714, 682, 698, and 714 cm−1 are in perfect agreement with both the data from the literature and experimental observation. The C-S vibration is clearly a pure mode, as Tables 6 and 7 demonstrate. Additionally, there is an equivalent correlation between the in-plane and out-of-plane C-S stretching vibration and experimental observations.

3.4.3 C=N Vibrations

The region 1672–1566 cm−1 is where the C=N stretching vibrations (Khokr, Arora, Kha, Kaushik, Saini, Husain, 2019; Mishra, Ghanavatkara, Malib, Qureshi, Chaudhari, Sekar, 2019) has been observed. For BT molecules, the corresponding bands in the IR spectra at 1634, 1488, 1541, and 1555 592 cm−1 are attributed to the C=N stretching vibration. Tables 6 and 7 display the bands that correspond to the C–C–C and C–S–C in-plane and out-of-plane bending modes of BT. According to normal coordinate analysis, there is a noticeable blending of C-H and C-C-C in-plane bending. Similarly, there is a large overlap between the C–H out of plane bending modes and the skeleton out of plane bending modes.

3.4.4 Ring Vibrations

The benzene ring's carbon–carbon stretching modes are predicted to lie between 1650 and 1200 cm−1, and they are typically not highly sensitive to minor substituent substitution; however, the frequency gets reduced by heavy halogens (El-Rayyes, Umar, 2005; El-Rayyes, Maung, 2005; El-Rayyes, Maung, 2004; El-Rayyes, 2003; El-Rayyes, 2003; Umar and El-Rayyes, 2024)]. The computed theoretical values for carbon-carbon stretching modes range from 1653 to 1208 cm−1. These values exhibit good agreement with previously published experimental data of 1654, 1612, and 1485 cm−1 (Khokr, Arora, Kha, Kaushik, Saini, Husain, 2019; Mishra, Ghanavatkara, Malib, Qureshi, Chaudhari, Sekar, 2019; Yagodzinska, Yagodzinski, Yablonski, 1980). The infrared band at 873 cm−1 corresponds to the BT ring's C–C–C in-plane bending vibrations. Together with the C-H in-plane bending vibrations, the C-C in-plane bending vibrations were observed as a combined vibrational mode. In the FTIR spectra for BT, the bands corresponding to C–C–C out-of-plane bending vibrations are seen at 585 and 531 cm−1.

3.4.5 C=O vibrations

In the infrared spectra of 1,3-benzothiazole-2-carboxaldehyde and 1,3-benzothiazole-2-carbonyl fluoride, the C=O stretching frequency is identified as the most intense band. The most stable trans conformers exhibit this line at 1859 cm−1, which was further blue-shifted for the COF group and identified at 1764 cm−1 for the CHO group (mode υ6).

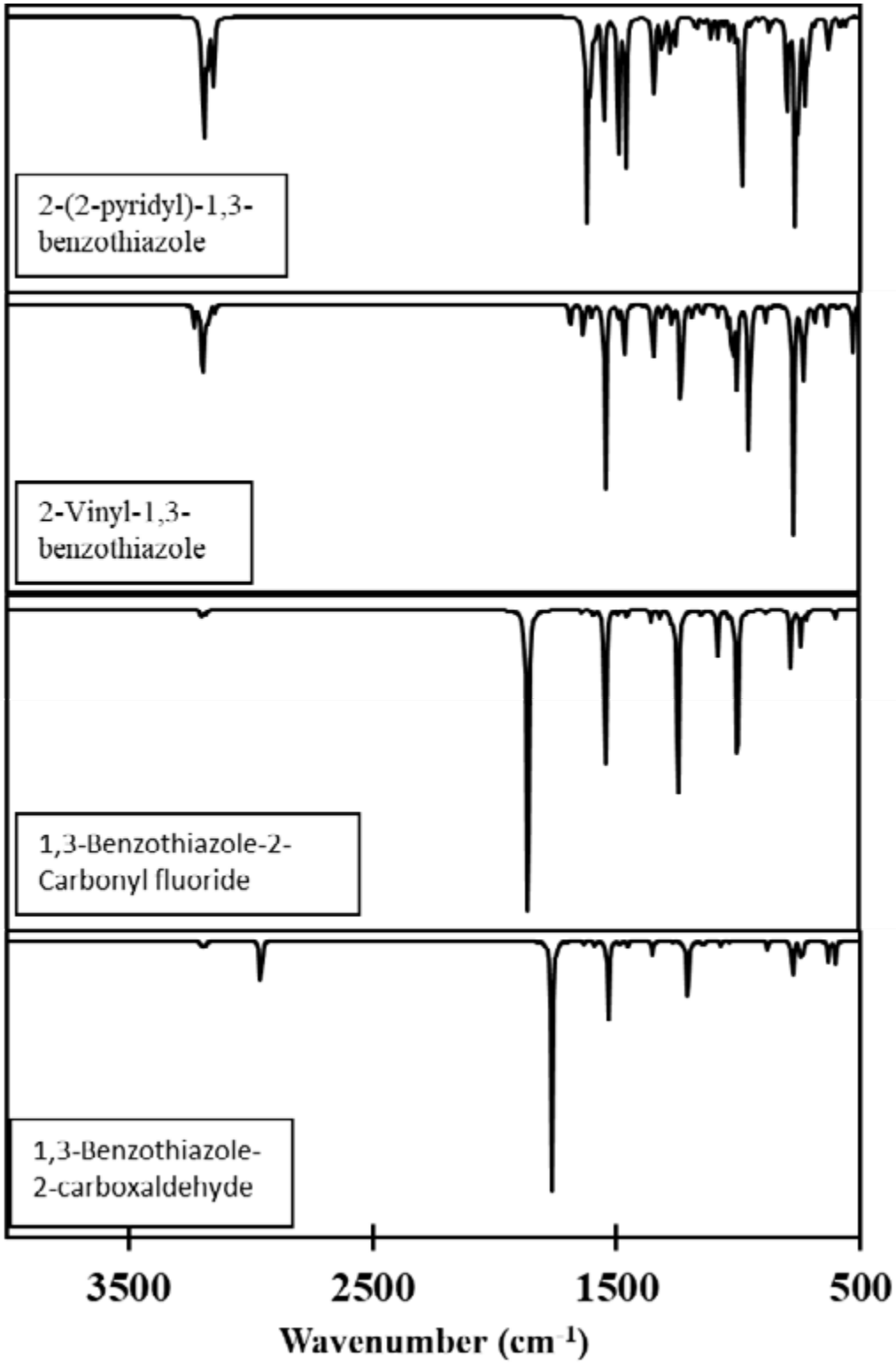

Figure 5: Vibrational IR spectra of substituted 1,3-BT molecules.

Table 6: Calculated vibrational wavenumber (cm^{-1}) for 1,3-Benzothiazole-2-carboxaldehyde and 1,3-Benzothiazole-2-carbonyl fluoride

No	1,3-Benzothiazole-2-carboxaldehyde			1,3-Benzothiazole-2-carbonyl fluoride		
	IR.[a]	Intensity[b]	Assignment[c] (PED ≥ 10%)	IR[a]	Intensity[b]	Assignment[c] (PED ≥ 10%)
ν1	3202	9.15	νCH(97)	3204	6.55	νCH(82)
ν2	3195	10.72	νCH(90)	3197	9.26	νCH(96)
ν3	3185	5.63	νCH(86)	3187	5.38	νCH(97)
ν4	3173	1.60	νCH(96)	3175	1.70	νCH(97)
ν5	2959	94.23	νCH(100)	1859	1024.48	νOC(100)
ν6	1764	860.19	νOC(93)	1635	10.45	νOC(93)
ν7	1634	11.20	νNC(67)	1588	12.94	νCC(63)
ν8	1588	13.32	νCC(63)	1539	423.21	νCC(55)
ν9	1534	316.16	νCC(71)	1488	14.46	νNC(69)
ν10	1488	14.08	νCC(79)	1453	32.49	νCC(34)+ δHCC(43)
ν11	1454	27.44	νCC(57)	1351	35.30	δCCC(14)+ δHCC(49)
ν12	1371	1.28	νCC(67)	1315	27.77	νSC(64)
ν13	1351	60.67	νNC(69)	1269	34.50	νNC(29)+ δHCC(49)
ν14	1309	0.01	νCC(64)	1242	895.00	νCC(14)+νNC(21)+δHCC(34)
ν15	1267	4.27	νSC(83)	1189	1.90	νCC(29)+νFC(17)+δOCF(13)+δCNC(12)
ν16	1208	415.55	νCC(37)+δCCN(39)	1145	24.57	νCC(18)+δHCC(56)
ν17	1187	15.85	δHCC(68)	1079	199.28	νCC24+δHCC(44)
ν18	1145	28.38	νCC(12)+δHCC(52)	1035	23.24	νSC(17)+δCCC(43)+δHCC(10)
ν19	1071	22.19	νSC(20)+δCCC(46)	999	0.05	νCC(59)+δHCC(18)
ν20	1034	7.88	νCC(67)+δHCC(21)	998	1005.22	τHCCC(76)
ν21	1001	0.67	δHCCS(68)+δOCCS(26)	965	5.75	νFC(43)+δCNC(26)
ν22	995	0.13	δHCCC(64)+τCCCC(11)	883	16.01	τHCCC(80)
ν23	963	6.39	δHCCC(79)	867	4.22	νCC(12)+νNC(16)+δCCC(32)
ν24	881	58.37	νNC(13)+δCCC(58)	777	309.97	HCCC(88)
ν25	867	3.23	τHCCC(83)	749	16.10	τHCCC(67)
ν26	777	260.21	τHCCC(69)+τCCCC(20)	736	58.89	τOCFC(78)+τCNSC(10)
ν27	746	100.31	δCCO(64)	735	146.54	δNCC(25)+δCCF(17)
ν28	738	137.41	τHCCC(43)+τCCCC(36)	715	48.01	τHCCC(20)+τCNSC(35)+τCCCC(16)
ν29	714	6.50	νSC(25)+δCCC(46)	698	9.33	νSC(27)+δCCC(43)
ν30	630	196.64	δCCC(28)+δCCN(31)	596	58.98	νFC(11)+δOCF(38)+δCNC(10)+δNCC(10)
ν31	602	236.60	δCCC(40)+ δCCN(18)	595	2.70	δCCC(56)
ν32	601	0.20	τCCCC(63)+τSCCC(13)	512	0.60	δCCC(56)+τSCCC(13)
ν33	510	1.81	νSC(25)+δSCC(21)+δCCC(28)			
ν34	505	5.91	δCCC(15)+τSCCC(58)			

[a] Calculated IR vibrational wavenumbers, cm^{-1}(scaled with 0.9619). [b] Calculated infrared intensities in km mol^{-1}.
[c] ν is stretching, δ is bending, and τ is torsion

Table 7: Calculated vibrational wavenumber (cm^{-1}) for 2-(2-Pyridyl) 1,3-benzothiazole and 2-Vinyl-1,3-benzothiazole.

No	2-(2-Pyridyl)-1,3-benzothiazole			2-Vinyl-1,3-benzothiazole		
	IR.[a]	Intensity[b]	Assignment[c] (PED ≥ 10%)	IR[a]	Intensity[b]	Assignment[c] (PED ≥ 10%) cccccccc
ν1	3211	2.37	νCH(93)	3229	6.69	ν(CH) 95
ν2	3198	15.88	νCH(97)	3200	10.19	ν(CH)93
ν3	3195	20.43	νCH(93)	3193	12.99	ν(CH)93
ν4	3191	19.38	νCH(96)	3182	5.87	ν(CH)92
ν5	3180	6.84	νCH(96)	3170	1.18	ν(CH)92
ν6	3175	10.30	νCH(94)	3169	2.87	ν(CH)96
ν7	3169	1.28	νCH(97)	3142	2.08	ν(CH)97
ν8	3155	27.76	νCH(93)	1683	7.57	ν(CC) 62+δ(HCC)10+δ(HCC)11
ν9	1635	6.55	νCC(61)+δHCC(11)	1630	7.78	ν(CC)51
ν10	1623	127.51	νCC(53)	1594	3.52	ν(CC)59 +δ(HCC) 11
ν11	1607	58.12	νCC(62)+δHCC(10)	1541	45.41	ν(SC)11 + ν(NC)63
ν12	1592	12.15	νCC(50)	1487	4.26	δ(HCC)20 +
ν13	1555	73.71	νNC(69)	1462	12.49	δ(HCC) 51+ ν(CC)14
ν14	1494	125.02	νCC(20)+δHCC(16)+δHCN(31)	1442	0.34	δ(HCC)68 + ν(NC)11
ν15	1486	9.62	νCC(29)+δHCC(46)	1346	14.71	ν(CC)64 + δ(HCC)29+δ(HCC)10
ν16	1464	100.07	δHCC(49)	1310	2.95	δ(HCC)10+δ(HCC) 71
ν17	1460	4.01	δHCC(56)	1302	0.45	δ(HCC)14+δ(HCC)59
ν18	1348	80.77	νCC(51)	1266	4.60	δ(CCN)34+ν(CC)10
ν19	1321	7.18	νNC(26)+δHCN(26)	1229	36.37	δ(CCN)17+δ(HCC)24+ν(CC)35
ν20	1313	26.62	νCC(22)	1184	2.90	δ(HCC)17+δ(HCC)66
ν21	1306	5.41	νNC(59)	1144	3.09	δ(HCC)24+δ(HCC)56
ν22	1279	34.04	νCC(18)+δHCC(27)	1077	2.74	ν(SC)48+δ(CCC)26
ν23	1261	23.83	νNC(28)+δHCC(10)	1038	5.11	ν(CC)19+ν(CC)67
ν24	1185	6.36	νCC(12)+δHCC(66)	1018	16.44	τ(HCCH)94
ν25	1172	14.26	νCC(11)+δHCC(73)	999	23.26	δ(HCC)62
ν26	1144	7.11	νCC(14) + δHCC(41)	986	0.00	τ(HCCC)93
ν27	1114	19.43	νNC(14)+νCC(19)+δHCC(46)	953	0.07	τ(HCCC)87
ν28	1085	18.88	νSC(16)+δCCC(32)	950	45.88	τ(HCCH)97
ν29	1065	6.06	νCC(29)+δCCC(25)	884	4.85	δ(CCC)15+ ν(SC)17+δ(CCC)47
ν30	1036	20.38	νCC(59)+δHCC(26)	862	0.86	τ(HCCS)93
ν31	1016	0.20	τHCCC(73)s	769	56.31	τ(HCCC)94
ν32	1012	29.82	νNC(29)+δCNC(13) +δCCC(41)	730	21.51	τ(CCCC)93
ν33	989	204.46	δCNC(44)	718	4.93	τ(HCCN)96
ν34	985	0.59	τHCCC(69)	716	2.20	ν(CC)53+δ(CCN)18
ν35	984	2.10	τHCCC(73)	682	6.11	ν(SC)14+ν(SC)53+δ(CCN)10
ν36	952	6.52	τHCCC(70)+τCCCC(17)	632	5.92	ν(NC)36+ν(CC)14+δ(HCC) 15
ν37	917	2.94	τHCCC-84	586	1.20	τ(HCCC)91
ν38	874	15.43	νNC(13)+δCCC(23)+δCCC(13)	525	11.65	δ(HCC)22+δ(HCC)52
ν39	860	3.48	τHCCC(84)	509	0.41	ν(CC)45+ν(CC)15+ν(CC)16
ν40	801	175.47	τHCCC(49)+τSCCC(17)τCCCN(20)			
ν41	769	284.52	τHCCC(64)+τCCCC(11)			
ν42	756	125.75	τHCCC(17) + τHCCC(24)+τCNCC(41)			
ν43	730	87.59	τHCCC(32)+τCCCC (40)			
ν44	725	71.84	δCCC(44)+δCCN(12)			
ν45	714	45.67	νSC(30)+δCCC(15)+δCCC(23)			
ν46	691	12.86	δCCC(17)+δCCC(11)+δCCC(16)+δCCN(13)			
ν47	633	47.67	δCCC(73)			
ν48	629	21.71	τSCCC(12)+τCCCC(39)+τCCCN(13)			
ν49	585	26.92	δCCN(11)+δCCC(17)+δCCC(13)+δCCC(19)			
ν50	561	15.78	τCCCC(54)			
ν51	511	0.47	νSC(26)+δCCC(47)			

[a] Calculated IR vibrational wavenumbers, cm^{-1}(scaled with 0.9619). [b] Calculated infrared intensities in km mol^{-1}.
[c] ν is stretching, δ is bending, and τ is torsion

4. Conclusion

The geometrical structure of four substituted 1,3-BT molecules have been optimized using the B3LYP/6-31G(d,p) method without any symmetry constraints. Simulated UV-vis and IR, spectra were used to describe the spectroscopic properties of the molecules. Excited state calculations were carried out using the Time Dependent-DFT/6-311++G(d,p) method.

1,3-BT is found to exist in two main conforms, the A form and the B form with the B form to be more stable than the A form conformer with A to B form rotational barrier ranging from 5.73 Kcal/mol to 9.78 Kcal/mol. Symmetry of the thiazole ring is distorted due to substitution effect, yielding ring angles smaller than 120° at the point of substitution.

UV-vis spectra, HOMO-LUMO energies and the global quantum chemical parameters were determined. Simulated IR spectra were determined with complete assignments of the vibrational frequencies. For substituted 1,3-BT molecules, the energy difference between HOMO and LUMO was determined to be between 4.70 and 3.95 eV which demonstrates that vinyl derivative is chemically

more stable structure with an energy gap of 4.70 eV, whereas formyl derivative is the least stable, having an energy gap of 3.95 eV.

Both VBT and BTC have the highest and lowest values of η that is 2.35 and 1.98 eV, respectively. In light of this, it is simple to conclude that formyl BT is the softest molecule and the most susceptible to charge transfer and chemical reactions. In comparison to other molecules, a molecule with a greater χ parameter is a superior electron acceptor. χ values for both VBT and BTCF derivatives were having the lowest and greatest values and were determined to be 4.37 and 5.16 eV, respectively. The presence of fluoride atom can be the main cause for the high χ parameters associated with COF derivatives. Values for χ parameters decrease for both vinyl and pyridyl derivatives due mainly to the electron donating power of the alkenyl and aryl groups.

DATA AVAILABILITY STATEMENT:

The data that support the findings of this study are available on request from the corresponding author.

CONFLICTS OF INTEREST:

The author declares no conflict of interest, financial or otherwise.

ACKNOWLEDGEMENT:

Support from Northern Border University is gratefully acknowledged.

5. REFERENCES

Fabiola T., Horacio L., Silvia E. Castillo-Blum, and Noráh B. (2008). Coordination behavior of benzimidazole, 2-substituted benzimidazoles and benzothiazoles, towards transition metal ions. Ark. 245-275. https://doi.org/10.3998/ark.5550190.0009.519

Mubarik A., Mahmood S. Hashmi, M.A. Ammar, Mutahir M., Ali, K., Bilal, M., Akhtar, N., Ashraf, G.A. (2022). Computational Study of Benzothiazole Derivatives for Conformational, Thermodynamic and Spectroscopic Features and Their Potential to Act as Antibacterials. Crystals, 12, 912. https://doi.org/10.3390/cryst12070912

Sathyanarayanmoorthi V., Karunathan R., and Kannappan V. (2013). Molecular Modeling and Spectroscopic Studies of Benzothiazole. J. of Chem., http://dx.doi.org/10.1155/2013/258519

Muhd Z., Mark L., Syahidah T, Ishak, A., Mohammad K. *(2018). Experimental and DFT Investigation on the Influence of Electron Donor-Acceptor on the Hydrogen Bonding Interactions of 1-(1,3-Benzothiazol-2- y1)-3-(R-benzoylthiourea). Sains Malay., 47(5): 923–929.* http://dx.doi.org/10.17576/jsm-2018-4705-07

Mabrouk A., Azazi A., Alimi K., (2010). On the properties of new benzothiazole derivatives for organic light emitting diodes (OLEDs): A comprehensive theoretical study. J. Phys. and Chem Solids 71, 1225-1235.

Zahradník P. (1990). Quantum-chemical study of electronic structure and transmission of substituent effects in benzothiazole derivatives. Chem. Papers 44 (2) 145–150.

Lucie A. Bédé, Mawa Koné, Guy R. M. Kon, Simplice C. S. Ouattara, Lamoussa Ouattara, El Hadji S. Bamba (2019). Tautomeric Equilibrium Modeling: Stability and Reactivity of Benzothiazole and Derivatives. Intern. J. Chem., 11(1), 84-95.

Sumit Tahlan, Sanjiv Kumar and Balasubramanian Narasimhan (2019). .Antimicrobial potential of 1H-benzo[d] imidazole scaffold: a review. BMC Chem.,13-18. https://doi.org/10.1186/s13065-019-0521-y

Xiaoyuan Chen, Frank J. Femia, John W. Babich, Jon Zubieta (2001). Spectroscopic and structural studies of complexes of the fac-[Re(NSN)(CO)3L]n_ type (NSN_2-(2-pyridyl)benzothiazole; L_Cl, Br, CF3SO3 _, CH3CN). Inorg. Chim. Acta, 314, 91–96.

Sana Tariq, Payal Kamboj, Mohammad Amir (2019). Therapeutic advancement of benzothiazole derivatives in the last decennial period. Arch Pharm Chem Life Sci., 352(1): e1800170. https://doi.org/10.1002/ardp.201800170.

Sukhbir L. Khokr, Kanika Arora, Shah A. Kha, Pawan Kaushik, Reetu Saini and Asif Husain (2019). Synthesis, Computational Studies and Anticonvulsant Activity of Novel Benzothiazole Coupled Sulfonamide Derivatives. Iran. J. Pharm. Res. 18 (1), 1-11.

Virendra R. Mishra, Chaitanny W. Ghanavatkara, Suraj N. Malib, Shahnawaz. Qureshi, Hemchandra K. Chaudhari, Nagaiyan Sekar (2019). Design, synthesis, antimicrobial activity and computational studies of novel azo linked substituted benzimidazole, benzoxazole and benzothiazole derivatives. Comp. Biol. Chem., 78, 330–337.

Yagodzinska E., Yagodzinski T., and Yablonski Z., (1980). Synthesis and Spectrometric Investigation of the Thioa.Mides of Thiazole- and Benzothiazole-2-Carboxylic Acids. Khim. Get. Soed., 9,1287.

Nancy Singhal, Anasuya Mishra, and Anindya Datta (2016). Excited-State Proton Transfer and Conformational Relaxation of 2-(4'-Pyridyl) benzimidazole in Nafion Films. Chem. Phys. Chem., 17, 3004 – 3009. https://doi.org/10.1002/cphc.201600546.

Milan Maji, Parbati Sengupta, Shyamal Kumar Chattopadhyay, Golam Mostafa, Schwalbe C. H., Saktiprosad Ghosh (2001). An unusual ruthenium(ii) complex of 2-(2-pyridyl)

benzothiazole. J. Coord. Chem, 54(1), 13-24. https://doi.org/10.1080/00958970108022626.

Giovanni Coni, Marcella Massacesi, Gustavo Ponticelli, Giovanna Puggioni and Costantino Putzolu (1987). Palladium (II) and platinum(II) chloride and bromide complexes with some 2-methylpyridyl- or methylquinolyl-benzimidazole, benzoxazole, or benzthiazole. Trans. Met. Chem., 12, 379-381.

Jitender K Malik, Manvi F. V., Nanjwade B. K., Sanjiv Singh, Pankaj Purohit, (2010). Review of the 2-Amino Substituted Benzothiazoles: Different Methods of the Synthesis. Der Pharm. Lett., 2 (1) 347-359.

Asaithambi Gomathi, Paranthaman Vijayan, Periasamy Viswanathamurthi, Shanmugam Suresh, Raju Nandhakumar, Takeshi Hashimoto (2017). Organoruthenium (II) compounds with pyridyl benzoxazole/ benzthiazole moiety: studies on DNA/ protein binding and enzyme mimetic activities. J. Coord. Chem., 70(10), 1645–1666. https://doi.org/10.1080/00958972.2017.1309649.

Milan Melnik, Peter Mikuš and Clive Eduard Holloway, (2013). Platinum organometallic compounds: classification and analysis of crystallographic and structural data of monomeric five and higher coordinated. Rev. Inorg. Chem., 33(1) 13–103. https://doi.org/10.1515/revic-2013-0001.

Kuramshina G. M., Vakula O. A., Vakula N. I., Majouga A. G., Senyavin V. M., Leonid G. Gorb, Jerzy Leszczynski (2016). Conformations vibrational spectra and force field of 1-methyl-2-(2-pyridyl)benzimidazole: experimental data and density functional theory investigation in comparison with 2-(2-pyridyl)benzimidazole", Struct. Chem.27, 209–219. https://doi.org/10.1007/s11224-015-0693-6.

Jitender K Malik, Manvi F. V., Nanjwade B. K., Sanjiv Singh, Pankaj Purohit, (2010). Review of the 2-Amino Substituted Benzothiazoles: Different Methods of the Synthesis. Der Pharm. Lett, 2 (1) 347-359.

Yuping Tong, Jing Fu, Juntao Ma, (2018). A theoretical investigation about the excited state behavior for 2-(6'-hydroxy-2'-pyridyl) benzimidazole: The water-assisted excited state proton transfer process. J. Chin. Chem. Soc. 65, 822–827. https://doi.org/10.1002/jccs.201700446.

Fatemeh Niknam, Peyman Hamidizadeh, Masoud Nabavizadeh, Fatemeh Niroomand, Jafar Hoseini, Peter Ford, Mahdi M. Abu-Omar (2019). Synthesis, structural characterization, and luminescence properties of mono and di-nuclear platinum(II) complexes containing 2-(2-pyridyl)-benzimidazole. Inorg. Chim. Acta 498, 119133. https://doi.org/10.1016/j.ica.2019.119133.

Xiao-Feng He, Christopher Vogels, Andreas Decken, Stephen Westcott (2004). Pyridyl benzimidazole, benzoxazole, and benzothiazole platinum complexes. Polyhed. 23, 155–160. https://doi.org/10.1016/j.poly.2003.09.020.

Frisch M.J., Trucks G.W., Schlegel H.B.,. Scuseria G.E, Robb M.A., Cheeseman J.R., Zakrzewski V.G., Montgomery J.A., Stratmann Jr., R.E., Burant J.C., Dapprich S., Millam J.M., Daniels A.D., Kudin K.N., Strain M.C., Frakas O., Tomasi J., Barone V., Cossi M., Cammi, Mennucci B., Pomelli C., Adamo C., Clifford S., Ochterski J., Petersson G.A., Ayala P.Y., Cui Q., Morokuma K., Malick D.K., Rabuck A.D., Raghavachari K., Foresman J.B., Cioslowski J., Ortiz J.V., Baboul A.G., Stefanov B.B., Liu G., Liashenko A., Piskorz P., Komaromi I., Gomperts R., Martin R.L., Fox D.T., Keith T., Al-Laham M.A., Peng C.Y., Nanayakkara A., Gonzalez C., Challacombe M., Gill P.M.W., Johnson B.G., Chen W., Wong W., Andres J.L., Head-Gordon M., Replogle E.S., Pople J.A.,(2003). GAUSSIAN 03, Revision B.01, Gaussian, Inc., Pittsburgh, PA.

Roy Dennington, Todd A. Keith, and John M. Millam, (2016). Gauss View, Version 6.1, Semichem Inc., Shawnee Mission, KS.

Jamroz M. H. (2004). Vibrational Energy Distribution Analysis. VEDA 4 Program, Warsaw.

El-Rayyes Ali, Yunusa Umar (2005). Density Functional Theoretical studies on Structures and Vibrational Spectra of Fluorovinyl Silanimines. Can. J. of Anal. Sci. Spect. (CJASS), 50, 175-189.

El-Rayyes Ali, Maung T. H., (2005). Excited state Phototautomerization of 8-amino-1-naphthol-3, 6-disulfonate in polar and acidic solutions. Can. J. of Anal. Sci. Spect. (CJASS), 50, 111-118.

El-Rayyes Ali, Maung T. H. (2004). Theoretical studies on the structure and hydrogen bonding of 8-amino-1-naphthol and its one water complex. J. Mol. Struct. (Theochem), 681, 9-13.

El-Rayyes Ali. A. (2003). Theoretical Studies on the Geometrical Structures and Vibrational Spectra of N-hydroxy-1-vinylsilanimines. J. Mol. Struct. (Theochem), 624, 181-190.

El-Rayyes Ali. A. (2003). Structure and vibrational assignments of the various modes of Nitro-, Nitrozo- and Aminosilanimines. J. Mol. Struct. (Theochem)), 634, 289-298.

Yunusa Umar, El-Rayyes Ali, (2024). Theoretical investigation of the vibrational and electronic properties of tetraphenylammonium and its boron, aluminum, gallium, carbon, silicon, germane, phosphorus and arsenic analogues. Comp. Theor. Chem, 1231, 114423.